Lagrangian descriptors for open maps

Gabriel G. Carlo[1,*] and F. Borondo[2,3,†]

[1]*Comisión Nacional de Energía Atómica, CONICET, Departamento de Física, Av. del Libertador 8250, 1429 Buenos Aires, Argentina*

[2]*Departamento de Química, Universidad Autónoma de Madrid, Cantoblanco, 28049 Madrid, Spain*

[3]*Instituto de Ciencias Matemáticas (ICMAT), Cantoblanco, 28049 Madrid, Spain*

(Received 23 October 2019; accepted 27 January 2020; published 14 February 2020)

We adapt the concept of Lagrangian descriptors, which have been recently introduced as efficient indicators of phase space structures in chaotic systems, to unveil the key features of open maps. We apply them to the open tribaker map, a paradigmatic example not only in classical but also in quantum chaos. Our definition allows us to identify in a very simple way the inner structure of the chaotic repeller, which is the fundamental invariant set that governs the dynamics of this system. The homoclinic tangles of periodic orbits (POs) that belong to this set are clearly found. This could also have important consequences for chaotic scattering and in the development of the semiclassical theory of short POs for open systems.

DOI: 10.1103/PhysRevE.101.022208

I. INTRODUCTION

Lagrangian descriptors (LDs) [1] are a recently introduced classical measure that has proven to be very useful for the identification of the stable and unstable manifolds of chaotic systems [2–4]. They have also been applied to unveiling the chaotic structure in phase space of molecules, in particular the LiCN one [5] that is described by a realistic potential in two and three dimensions. This study has demonstrated the ability of LDs to overcome the difficulty posed by higher dimensionality to other methods such as obtaining a Poincaré surface of section. Also, LDs have been successfully implemented [6] within the so-called geometric transition state theory to the identification of recrossing-free dividing surfaces, thus helping in the computation of chemical reaction rates, and the reactive islands that account for nonstatistical behavior in chemical reactions [7]. Moreover, the concept has been adapted to discrete dynamical systems such as two-dimensional area preserving maps [8], under the name of discrete LDs. In this work the singular sets of LDs have been associated to the invariant manifolds of some prototypical maps and a chaotic repeller has been identified. As an interesting example of this method, LDs have been successfully applied to the Arnold's cat map [9] and its invariant manifolds have been easily described. This idea was recently extended to unbounded maps [10].

In this paper, we introduce a measure that is closely related to the original LDs but modified in such a way that makes it specially suitable to uncover the structure embedded in the repellers that characterize open systems [11]. Instead of the union of the stable and unstable manifold to which the original LD definition is more related, the prevailing object in the phase space of scattering [12] or projectively open systems, which are not area preserving is the set of nonescaping trajectories in the past and future. For that reason the LDs concept needs to be adapted to reveal the intersection of these manifolds.

We focus on open maps on the torus and we take the open tribaker map as a paradigmatic benchmark example. The simplest way to make a map open consists in eliminating the trajectories going through an opening in phase space, which can be any region of finite area [13]. Once a propagated initial condition falls into the opening, it stops being propagated and it is removed. Of course, the dynamics is not conservative since the open map acts by first removing points in the opening and then evolving the remaining ones according to the closed map. For long times, this leaves just a repeller, which is a fractal invariant set. Nevertheless, reflection mechanisms at the boundaries are usually more complicated than a complete opening [14], and they may exhibit many interesting mathematical consequences such as in optical microdisk cavities with boundary deformations [15]. In these latter apparently weakly open systems pronounced non-Hermitian phenomena appear. This leads us to consider in this work a function depending on a reflectivity R, which rules the way in which the classical trajectories arriving at the opening are only partially reflected. We study two cases, namely a (discontinuous) constant reflectivity function, and another of the Fermi-Dirac type that makes the boundaries of the opening smooth.

We have found that our modified LDs are very good indicators for the homoclinic tangles associated to POs, which are not easy to describe in general. In particular, the short POs and their homoclinic associates are readily localized with this measure. From the classical point of view, this is potentially very useful in the theory of chaotic scattering [16,17]. Moreover, it has applicability in the semiclassical theory of short POs [18–22], and the study of the morphology of chaotic eigenstates [23].

This is how the paper is organized. In Sec. II we define the Lagrangian descriptors for open maps, and describe the open tribaker map together with its main properties. In Sec. III

*carlo@tandar.cnea.gov.ar

†f.borondo@uam.es

we apply this definition to uncover the underlying structure of classical repellers, explaining our findings by using symbolic dynamics. Finally, our concluding remarks are presented in Sec. IV.

II. LAGRANGIAN DESCRIPTORS FOR OPEN MAPS

Essential properties of generic dynamical systems are well described by maps [24–26], and then they have been widely used as prototypical models of chaos. If we consider a two-dimensional phase space (canonical variables q and p) with an opening, i.e., a region through which trajectories can escape, we have open maps. These kinds of transformations of the two-torus can be used to model chaotic scattering [16] and microlasers [27], for example. The main invariant set that rules their properties is the so-called repeller, which has fractal dimension, and it is formed by the intersection of the forward and backward trapped sets. These, in turn, are made of the trajectories that never escape either in the past or in the future, respectively. The repeller is usually characterized by means of a measure $\mu(X_i)$ at each phase space region X_i determined by the average intensity I_t when $t \to \infty$ of a number $N_{\rm ic}$ of initial conditions randomly chosen inside X_i. The initial intensity is $I_0 = 1$ for each trajectory, and it is decreased as $I_{t+1} = F_R(q, p)I_t$ each time it hits the opening [28] [$F_R(q, p)$ is the reflectivity function to be defined in what follows]. A finite-time approximation to the measure for X_i can be defined by $\mu^b_{t,i} = \langle I_{t,i}\rangle / \sum_i \langle I_{t,i}\rangle$ where the average is performed over the initial conditions in the given phase space region. This is the finite-time backwards trapped set of open maps, and if evolved backwards $\mu^f_{t,i}$ is obtained, which is the forward trapped set. The intersection $\mu^b_{t,i} \cap \mu^f_{t,i}$ is the finite-time repeller $\mu_{t,i}$.

However, this quantity does not give information regarding the inner structure of the invariant set. In order to throw light on this, we modify the original definition of discrete LDs for area preserving maps. If we consider a trajectory $\{q_t, p_t\}^{t=T}_{t=-T}$, where $t \in \mathbb{N}$, discrete LDs were defined in Ref. [8] as

$$\mathrm{LD}_a = \sum_{t=-T}^{t=T-1} |q_{t+1} - q_t|^a + |p_{t+1} - p_t|^a, \tag{1}$$

with $a \leqslant 1$. As the repeller is the intersection of the backward and forward trapped sets, we define now the LDs for open maps (which we call LDO from now on) as

$$\mathrm{LDO}_a = \sum_{t=-T}^{t=-1} (|q_{t+1} - q_t|^a + |p_{t+1} - p_t|^a) I_t \times \sum_{t=0}^{t=T-1} (|q_{t+1} - q_t|^a + |p_{t+1} - p_t|^a) I_t, \tag{2}$$

with $a = -0.3$ throughout this work (we drop the subscript a in the following). Notice that we require $a < 0$ in order to provide a direct comparison with the measure μ. This is because μ is enhanced in those regions of phase space from which initial conditions do not escape, in particular POs belonging to the repeller. In fact, by taking $a < 0$ the highest values of LDO_a are located at these latter (and their manifolds). We take a $3^5 \times 3^5$ square grid on the torus with $N_{\rm ic} = 10^3$ at each region X_i so defined; also we normalize the LDOs to 1.

The paradigmatic tribaker map is the model chosen for our studies since this is one of the simplest chaotic maps, which can be described by a ternary Bernoulli shift. In fact, the original baker map, named like this by Halmos [29], is remarkable: all features of chaos are present in it, nevertheless all its classical structures have an analytical description, in contrast with other paradigmatic models of chaos. Its definition is purely geometrical and can be seen as the action of a baker compressing the dough in the p direction and stretching it along q and finally cutting and stacking to render it mixing. This translates into p and q being the stable and unstable directions, respectively. It has also been used as a model for high-dimensional chaos [30]. Formally, The tribaker map is an area-preserving, uniformly hyperbolic, piecewise-linear, and invertible map with Lyapunov exponent $\lambda = \ln 3$.

Moreover, the openings can be chosen to follow the stable and unstable manifolds. The open map is then simply the composition of the closed tribaker transformation

$$\mathcal{B}(q, p) = \begin{cases} (3q, p/3) & \text{if } 0 \leqslant q < 1/3 \\ (3q - 1, (p + 1)/3) & \text{if } 1/3 \leqslant q < 2/3 \\ (3q - 2, (p + 2)/3) & \text{if } 2/3 \leqslant q < 1 \end{cases} \tag{3}$$

with the selected opening. Notice that the opening mechanisms are not always as simple as a constant discontinuous function of q and p [22]. In fact, partially open maps are those in which the opening reflects some of the trajectories that arrive at it [23]. In this paper we study two different functions of the phase space $F_R(q, p)$, where R is the parameter that determines a transition between a given minimum amount of reflection $R = 0$ and the closed map ($R = 1$). We define the opening region as the domain $1/3 < q < 2/3$ of the reflectivity function F_R. We take a constant function given by the value of R in the opening and 1 elsewhere. In this case, we obtain a complete opening for $R = 0$; in all the other cases some amount of the incoming orbits is reflected. The other reflectivity that is considered in this work is given by

$$F_R(q, p) = \begin{cases} (1 - R)/\{1 + \exp[-A(q - B)]\} + R \\ \text{if } q > 1/2 \\ (1 - R)/(1 + \exp\{-A[(1 - q) - B]\}) + R \\ \text{if } q < 1/2, \end{cases} \tag{4}$$

which consists of a Fermi-Dirac-type step function. We fix $A = 120$ and $B = 0.63$, which gives a value of approximately 1 at $q = 1/3$ and $q = 2/3$, and the minimum value R at the middle of the opening. This function represents a smoothing of the hard step considered in the previous case. In order to clarify the shape of both reflectivity functions we show them in Fig. 1.

The symbolic dynamics associated to the map action is very simple, being given by a Bernoulli shift in the ternary representation of $q = 0.\epsilon_0\epsilon_1\epsilon_2\ldots$ and $p = 0.\epsilon_{-1}\epsilon_{-2}\epsilon_{-3}\ldots$ where $\epsilon_i = 0, 1, 2$, as

$$(p|q) = \ldots\epsilon_{-2}\epsilon_{-1}.\epsilon_0\epsilon_1\ldots \xrightarrow{\mathcal{B}} (p'|q') = \ldots\epsilon_{-2}\epsilon_{-1}\epsilon_0.\epsilon_1\ldots. \tag{5}$$

Hence, applying the map simply implies to move the decimal point one position to the right (this is merely a question

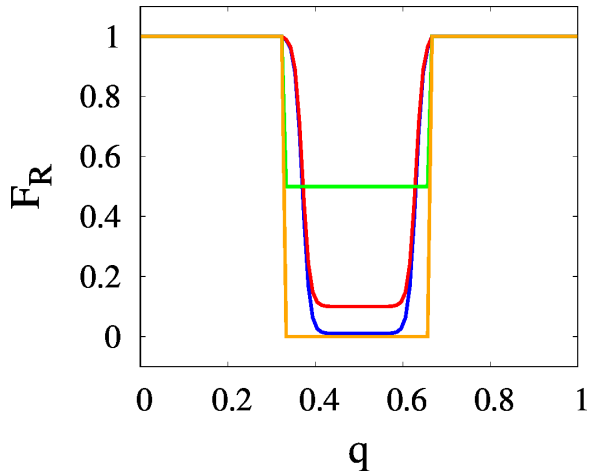

FIG. 1. Reflectivity functions $F_R(q, p)$ used in our study as a function of q. Dark gray (blue) and gray (red) lines correspond to the Fermi-Dirac type for $R = 0.01$ and $R = 0.1$, respectively. Light (orange) and lighter (green) lines to the discontinuous function for $R = 0$ and $R = 0.5$.

of q and p definition in terms of the symbolic sequence). For the opening region that we have chosen and in the case of the discontinuous function, it is clear that the equivalent in ternary notation can be obtained by using open symbols $\tilde{\epsilon}$ with forbidden value 1 ($\tilde{\epsilon} = 0, 2$). We consider only this possibility in order to study all reflectivity situations (and of course all symbols for the closed map case). One of the advantages of having such a simple symbolic dynamics (which unfortunately is not the usual situation) is that POs and their associated homoclinic tangles can be computed very easily. In this case, POs are simply given by an infinite repetition of a string of symbols $\nu = \epsilon_0 \dots \epsilon_L$, where L is the period. The homoclinic tangle of ν, which is formed by the orbits that belong to both the stable and unstable manifolds of the PO, can be approximated at short times by strings of the form $\nu_H^e = \nu \dots \nu\epsilon^e\nu \dots \nu$, where the orbit ν is repeated e times at each end, and the homoclinic excursions strings ϵ^e go from length 1 up to $e \in \mathbb{N}$.

III. RESULTS

How does the description of the repeller by means of the measure μ compare with the LDOs? To answer this question we first examine the results of Fig. 2. In it, we show in the top row the finite-time repeller measure $\mu_{t,i}$ at $t = 10$ obtained for the constant reflectivity function, while in the second to fourth rows the corresponding LDOs for the first, second, and third powers of the map with $T = 15$ are displayed; panels in the left and right columns correspond to $R = 0$ and $R = 0.5$, respectively. The choice of $T = 15$ is based on numerical evidence, this value provides with a very good identification of the POs and the manifolds associated to them (a longer evolution is not only computationally challenging but it does not contribute to obtain better results). Several comments are in order. First, it is clearly observed that the LDOs are peaked at the only surviving POs of period 1, 2, and 3 in the repeller, marked with (blue) dark gray circles in the figure. Second,

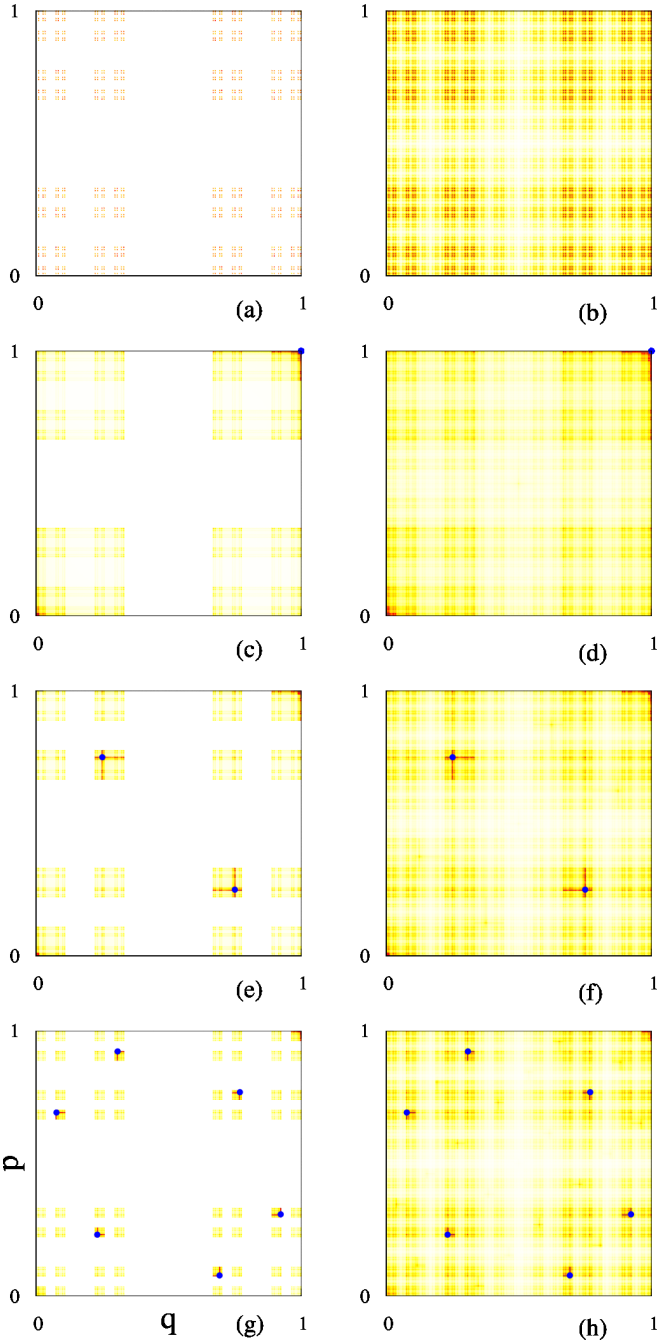

FIG. 2. Finite-time repeller measure $\mu_{t,i}$ for the discontinuous reflectivity open tribaker map on the two-torus at $t = 10$ with (a) $R = 0$ and (b) $R = 0.5$. Corresponding values of the LDOs for the (c)–(d) first, (e)–(f) second, and (g)–(h) third power of the same map for $T = 15$. The POs are marked by (blue) dark gray circles.

a substantial enhancement of the distribution around these POs is observed, while we do not find a significant difference with respect to this enhancement for the two values of the reflectivity, despite the fact that $R = 0.5$ is only halfway to the closed map. Finally, what is left from the stable and unstable manifolds is clearly shown by the LDOs, whose values go to a smaller scale with growing period. What is more important, this suggests the way in which trajectories escape through the map opening.

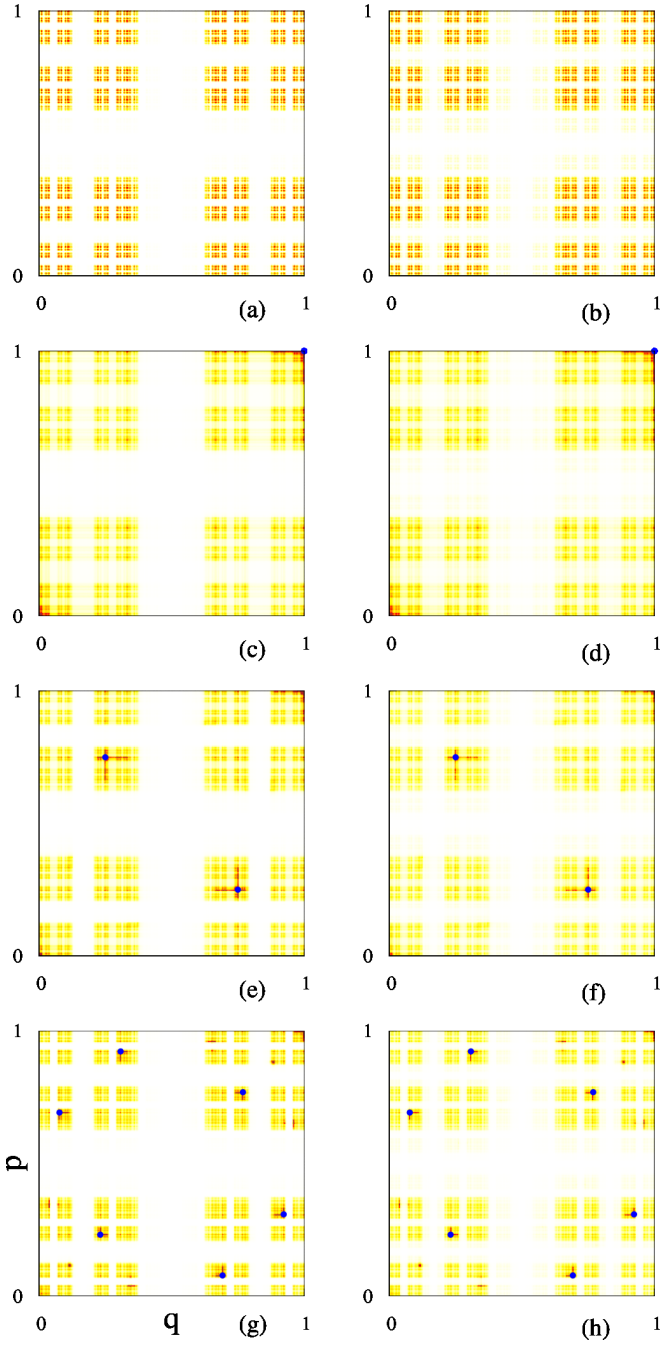

FIG. 3. Finite-time repeller measure $\mu_{t,i}$ for the Fermi-Dirac type reflectivity open tribaker map on the two-torus at $t = 10$ with (a) $R = 0.01$ and (b) $R = 0.1$. Corresponding values of the LDOs for the (c)–(d) first, (e)–(f) second, and (g)–(h) third power of the same map for $T = 15$. The POs are marked by (blue) dark gray circles.

In the case of the Fermi-Dirac-type reflectivity (see results in Fig. 3), we obtain the same kind of behavior, namely the LDOs peak around the POs of each map, and there is essentially the same manifold structure for both $R = 0.01$ and $R = 0.1$. For this function, we have chosen two low reflectivities to compare how different the morphology of LDOs is in this regime. It is evident that though there is an order of magnitude difference between both R values the map is essentially open with no significant discrepancies.

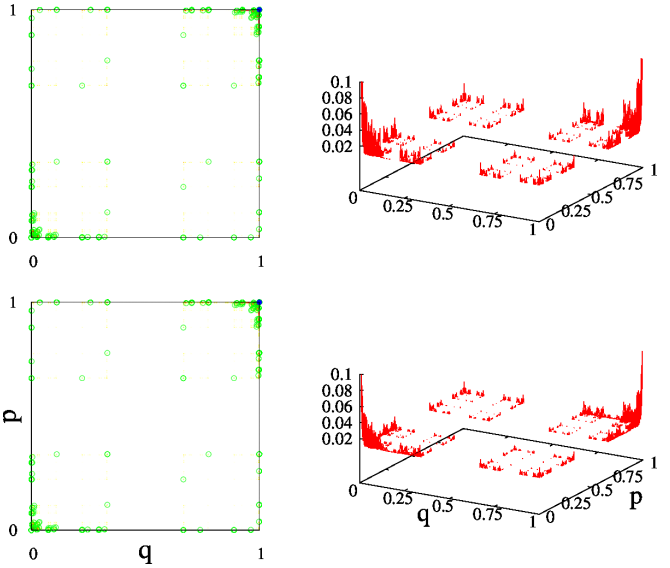

FIG. 4. LDO for the first power of the discontinuous opening tribaker map for $R = 0$ (top), and $R = 0.5$ bottom. On the left panels we show density plots together with the short-time homoclinic tangle approximation with empty (green) light gray circles. The POs are marked by (blue) dark gray circles. On the right the corresponding three dimensional views are shown. In all cases data below 0.01 have been discarded.

We next analyze and compare the effect of both openings for different powers of the map. Looking at Figs. 4 and 5 it is clear that the peaks are localized at the origin (or alternatively at the opposite corner identified with it in the torus), but

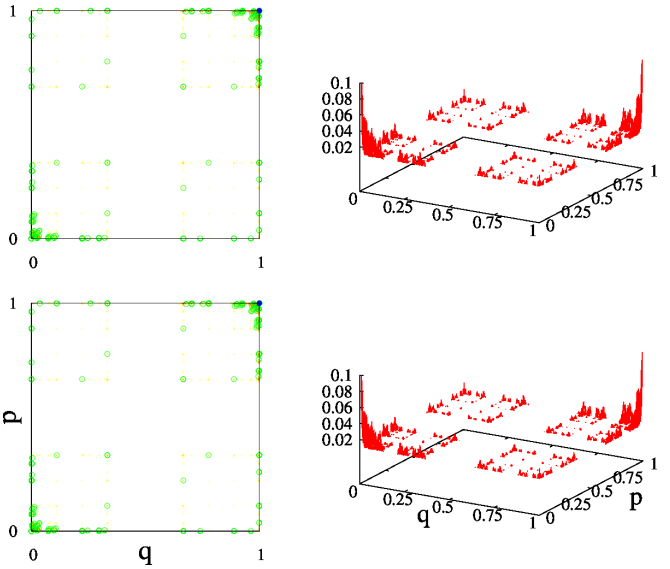

FIG. 5. LDO for the first power of the Fermi-Dirac type opening tribaker map for $R = 0.01$ (top), and $R = 0.1$ bottom. On the left panels we show density plots together with the short-time homoclinic tangle approximation with empty (green) light gray circles. The POs are marked by (blue) dark gray circles. On the right the corresponding three dimensional views are shown. In all cases data below 0.01 have been discarded.

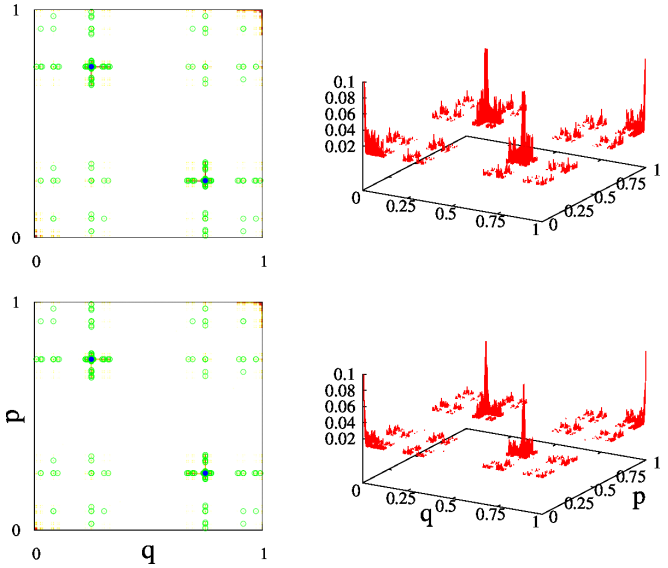

FIG. 6. Same as Fig. 4 but for the second power of the corresponding map.

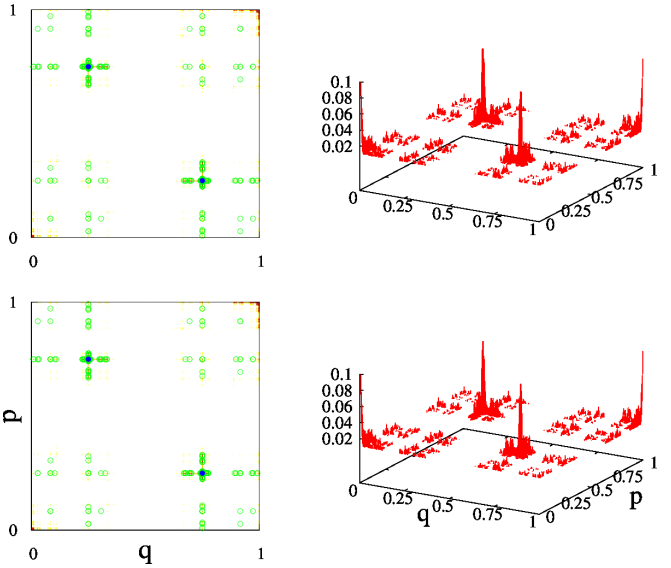

FIG. 7. Same as Fig. 5 but for the second power of the corresponding map.

also on a region around it. On the left columns, we can see the density plots (this density corresponds to the LDOs), where too small values have been discarded for clarity. We plot superimposed the PO at $\{1, 1\}$ [(blue) dark gray circles] and the short-time approximation to the homoclinic tangle [empty (green) light gray circles] obtained with $e = 3$. It is clear that the enhanced region agrees very well with the location of this tangle. In fact, if we look at the corresponding three-dimensional views on the right columns a clear contrast between the values on the homoclinic tangle and the rest of the torus can be appreciated. It is remarkable that there is no big difference among the distributions for the discontinuous opening for $R = 0.5$ and the Fermi-Dirac cases, though the completely open case shows more contrast.

Results for the second power of the maps are shown in Figs. 6 and 7. The same behavior as in the case of the first power is found. Notice that the period 1 PO is a PO of this map so we find it again. Also, the only surviving period 2 orbit is clearly signaled by the LDOs, and moreover we can verify with the help of symbolic dynamics that its homoclinic tangle is very well described. Again, there is a higher contrast between the region associated with the short-time approximation to the homoclinic tangle and the rest of the two-torus domain in the completely open scenario, i.e., the discontinuous opening case for $R = 0$.

Finally, from Figs. 8 and 9 it is clear that the third power of the maps shows the same behavior found in the two previous cases. Indeed, there is a clear enhancement of the LDOs around the surviving period 3 orbits. This time, we assume that it is the short-time homoclinic tangle, but the calculations even with the help of symbolic dynamics become computationally difficult. However, this result shows the power of the LDOs in order to unveil the exact morphology of these sets in generic systems. We notice a small but interesting difference between the discontinuous case and the Fermi-Dirac one. Some peaks on POs inside the opening can be found and this could be ascribed to their location near the border of this region, and the smoothing of this boundary performed by the reflectivity function. We point out that this could give important information on the role played by the POs outside the repeller in the escape mechanism, with seemingly nontrivial semiclassical consequences.

What happens if we apply our definition of LDOs to the closed map? In principle, the motivation for adapting the original LDs was to unveil the inner structure of the repellers. But the LDOs definition when $I_t = 1$ for all times can also be useful to locate the homoclinic tangle of POs of closed systems. In Fig. 10 we show the density plots for the first (top row) and the second (bottom row) power of the closed map. On the left column all data values were taken into account and a clear enhancement around the POs can be appreciated.

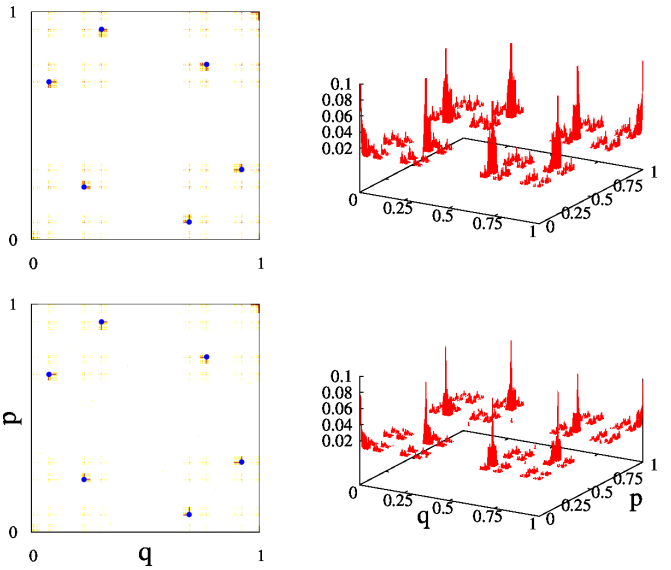

FIG. 8. Same as Fig. 4 but for the third power of the corresponding map (no homoclinic tangle approximation).

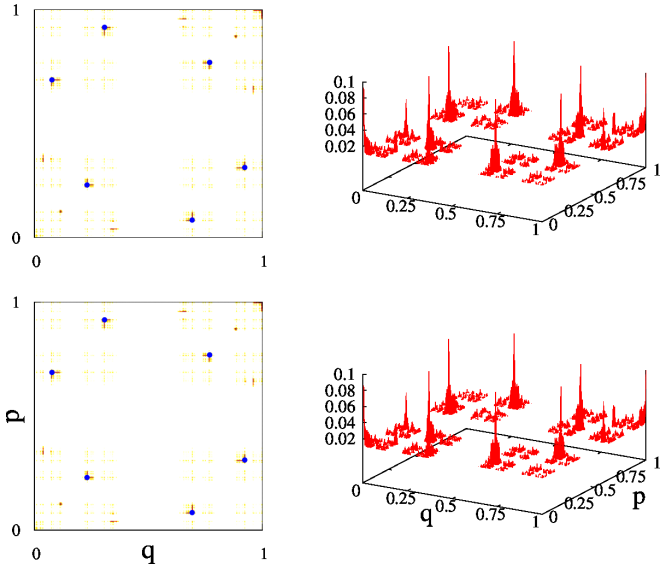

FIG. 9. Same as Fig. 5 but for the third power of the corresponding map (no homoclinic tangle approximation).

On the right column we discard the lowest values of LDOs and superimpose the short-time approximation to the closed homoclinic tangle for the same two orbits of period 1 and 2 that survive in the repeller. Of course, now there are more orbits, but the description of the homoclinic sets is still valid.

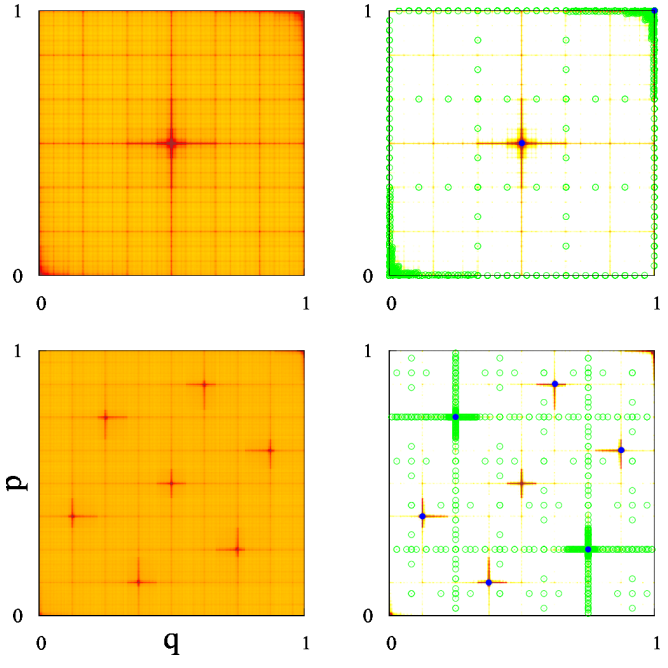

FIG. 10. LDOs for the first (top row) and second (bottom row) powers of the closed tribaker map. On the left we show the corresponding density plots considering all data values while, on the right we have discarded those below 0.0045. Also on the right we show the closed short-time homoclinic tangle approximations of the same period 1 and 2 POs considered in the previous figures with empty (green) light gray circles. The POs are marked by (blue) dark gray circles.

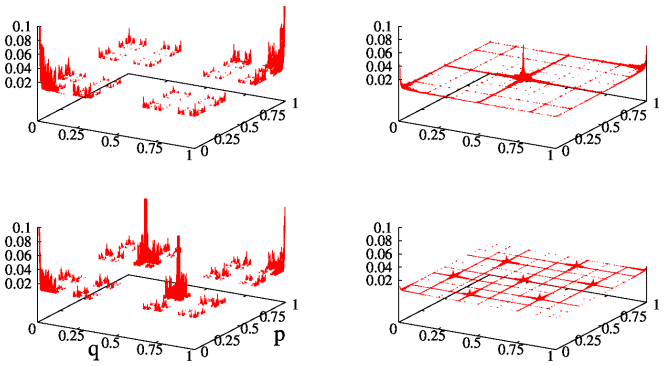

FIG. 11. Three-dimensional views of the LDOs for the first (top row) and second (bottom row) powers of the tribaker map. On the left column we show the results for the discontinuous opening case with $R = 0$, and on the right one for the closed map ($R = 1$).

However, if we look at Fig. 11 it becomes clear that the high contrast obtained for the open case is completely lost in the closed map. This result is due to the fact that the ratio of open to closed homoclinic orbits is given by $(2/3)^e$, which vanishes for $e \to \infty$. This makes LDOs strongly peak on them for the open case, while in the closed scenario we have a more homogeneous situation. More importantly, this underlines in a very bold way the special suitability of the LDOs concept to uncover the details of repellers, including the overwhelming effect that any kind of opening has on its inner structure, specially on the remains of the homoclinic tangles.

IV. CONCLUSIONS

The recently introduced concept of LDs has proven to be very useful for unveiling the dynamical structures embedded in chaotic phase space. In fact, the manifolds are obtained from very simple calculations, actually trajectory and simple sums computations, which are more friendly to users outside the nonlinear dynamics field. It is very amenable to numerical implementations and remarkably simpler than other methods for computational analysis of complex systems. Its definition in the discrete dynamical case has allowed to identify the stable and unstable manifolds associated to the POs of closed maps (autonomous and not), including the paradigmatic case of the Arnold's cat map.

We have successfully adapted this measure for open maps on the torus, defining the LDOs. With them, we have been able to identify the POs and the remains of the stable and unstable manifolds surviving in the repeller of the open tribaker map in two reflectivity function cases, i.e., the discontinuous and the Fermi-Dirac types of openings. This gives hints on possible applications for the study of trajectory escape mechanisms in more complicated systems. Moreover, with the aid of the very simple symbolic dynamics available for the tribaker map we could verify that our measure strongly peaks on the homoclinic tangles belonging to the POs. The high contrast between the values of the LDOs on these sets and the rest of the two-torus not only allows for a very precise characterization of them, but it is indicative of the way in which the homoclinic circuits [31] are truncated by the opening. It is important

to notice that in both opening scenarios the structure of the repeller is essentially the same. This is an important result in that it provides a qualitative but unambiguous indicator of openness for a given map. As a matter of fact, this high contrast is almost completely lost in the closed case, where homoclinic orbits exponentially outnumber those belonging to the repeller. We point out that these sets are not easy to identify in generic cases. Minor details associated to the kind of opening were also visualized, such as the relevant role played in the escape from the repeller by POs that do not belong to it when using the Fermi-Dirac type of reflectivity. We notice that some analytical calculations along the lines of Ref. [9] are amenable to our scenario. However, in this work we have focused on showing the power of our definition to unveiling classical structures embedded in the repeller.

All these results lead us to conclude that this work opens numerous possibilities for future research. On the one hand, chaotic scattering theory, where the homoclinic tangles play an essential role could receive new insights from LDOs characterization of generic complex systems. On the other hand, the semiclassical theory of short POs for open systems, which has raised the question of the role played by the POs outside of the repeller in the eigenfunctions description, could also greatly benefit from the use of LDOs to identify regions of higher relevance. In fact, the search for scar functions contributions from these phase space regions could simplify the current POs selection criteria. The first hint in this direction is given by Fig. 9 where some enhancement of the LDOs for the Fermi-Dirac opening region suggests to investigate scar functions constructed by the associated POs. Evaluating the semiclassical theory performance with or without these functions will be our next step.

ACKNOWLEDGMENTS

Support from CONICET is gratefully acknowledged. This research has also been partially funded by the Spanish Ministry of Science, Innovation and Universities, Gobierno de España under Contract No. PGC2018-093854-B-I00, and by ICMAT Severo Ochoa under Contract No. SEV-2015-0554.

[1] J. A. Jiménez-Madrid and A. M. Mancho, Chaos **19**, 013111 (2009).
[2] A. M. Mancho, S. Wiggins, J. Curbelo, and C. Mendoza, Commun. Nonlinear Sci. Num. Simul. **18**, 3530 (2013).
[3] F. Balibrea-Iniesta, C. Lopesino, S. Wiggins, and A. M. Mancho, Int. J. Bifur. Chaos **25**, 1550172 (2015).
[4] C. Lopesino, F. Balibrea-Iniesta, S. Wiggins, and A. M. Mancho, Int. J. Bifur. Chaos **25**, 1550184 (2015).
[5] F. Revuelta, R. M. Benito, and F. Borondo, Phys. Rev. E **99**, 032221 (2019).
[6] A. Junginger, G. T. Craven, T. Bartsch, F. Revuelta, F. Borondo, R. M. Benito, and R. Hernandez, Phys. Chem. Chem. Phys. **18**, 30270 (2016).
[7] S. Patra and S. Keshavamurthy, Phys. Chem. Chem. Phys. **20**, 4970 (2018).
[8] C. Lopesino, F. Balibrea-Iniesta, S. Wiggins, and A. M. Mancho, Commun. Nonlinear Sci. Num. Simul. **27**, 40 (2015).
[9] V. J. García-Garrido, F. Balibrea-Iniesta, S. Wiggins, A. M. Mancho, and C. Lopesino, Regul. Chaotic Dyn. **23**, 751 (2018).
[10] V. J. García-Garrido, Int. J. Bifurc. Chaos Appl. Sci. Eng. (unpublished).
[11] K. Clauß, E. G. Altmann, A. Bäcker, and R. Ketzmerick, Phys. Rev. E **100**, 052205 (2019).
[12] J. Seoane and M. A. F. Sanjuán, Rep. Prog. Phys. **76**, 016001 (2013); B. R. Hunt, E. Ott, and J. A. Yorke, Phys. Rev. E **54**, 4819 (1996); Y.-C. Lai and T. Tel, *Transient Chaos, Complex Dynamics on Finite-Time Scales* (Springer, New York, 2011); M. A. F. Sanjuán, T. Horita, and K. Aihara, Chaos **13**, 17 (2003).
[13] M. Novaes, J. Phys. A **46**, 143001 (2013).
[14] J. Wiersig and J. Main, Phys. Rev. E **77**, 036205 (2008).
[15] J. Kullig and J. Wiersig, New J. Phys. **18**, 015005 (2016).
[16] C. Jung, O. Merlo, T. H. Seligman, and W. P. K. Zapfe, New J. Phys. **12**, 103021 (2010).
[17] S. Wiggins, *Normally Hyperbolic Invariant Manifolds in Dynamical Systems* (Springer-Verlag, New York, 1994).
[18] M. Novaes, J. M. Pedrosa, D. Wisniacki, G. G. Carlo, and J. P. Keating, Phys. Rev. E **80**, 035202(R) (2009).
[19] L. Ermann, G. G. Carlo, and M. Saraceno, Phys. Rev. Lett. **103**, 054102 (2009).
[20] J. M. Pedrosa, D. Wisniacki, G. G. Carlo, and M. Novaes, Phys. Rev. E **85**, 036203 (2012).
[21] G. G. Carlo, D. A. Wisniacki, L. Ermann, R. M. Benito, and F. Borondo, Phys. Rev. E **87**, 012909 (2013).
[22] G. G. Carlo, R. M. Benito, and F. Borondo, Phys. Rev. E **94**, 012222 (2016).
[23] C. A. Prado, G. G. Carlo, R. M. Benito, and F. Borondo, Phys. Rev. E **97**, 042211 (2018).
[24] M. B. Dematos and A. M. O. Dealmeida, Ann. Phys. (NY) **237**, 46 (1995).
[25] J. H. Hannay and M. V. Berry, Physica D (Amsterdam) **1**, 267 (1980).
[26] M. Degli Espositi and B. Winn, J. Phys. A **38**, 5895 (2005).
[27] H. Cao and J. Wiersig, Rev. Mod. Phys. **87**, 61 (2015).
[28] J. U. Nöckel and D. A. Stone, Nature (London) **385**, 45 (1997).
[29] P. R. Halmos, *Lectures on Ergodic Theory* (Chelsea Publishing Company, New York, 1956).
[30] Y. Saiki, M. A. F. Sanjuán, and J. A. Yorke, Chaos **28**, 103110 (2018).
[31] E. L. Sibert III, E. Vergini, R. M. Benito, and F. Borondo, New J. Phys. **10**, 053016 (2008).